New Journal of Chemistry

Supporting Information

Hydrogen photogeneration catalyzed by a cobalt complex of pentadentate aminopyridine-based ligand

Xiaowei Song [a,b], Huimin Wen [a], Chengbing Ma [a], Hui Chen [a] and Changneng Chen [a*]

[a] State Key Laboratory of Structural Chemistry, Fujian Institute of Research on the Structure of Matter, Chinese Academy of Sciences, Fuzhou, Fujian 350002, P. R. China;

[b] University of Chinese Academy of Sciences, Beijing, 100049, China

E-mail: ccn@fjirsm.ac.cn.

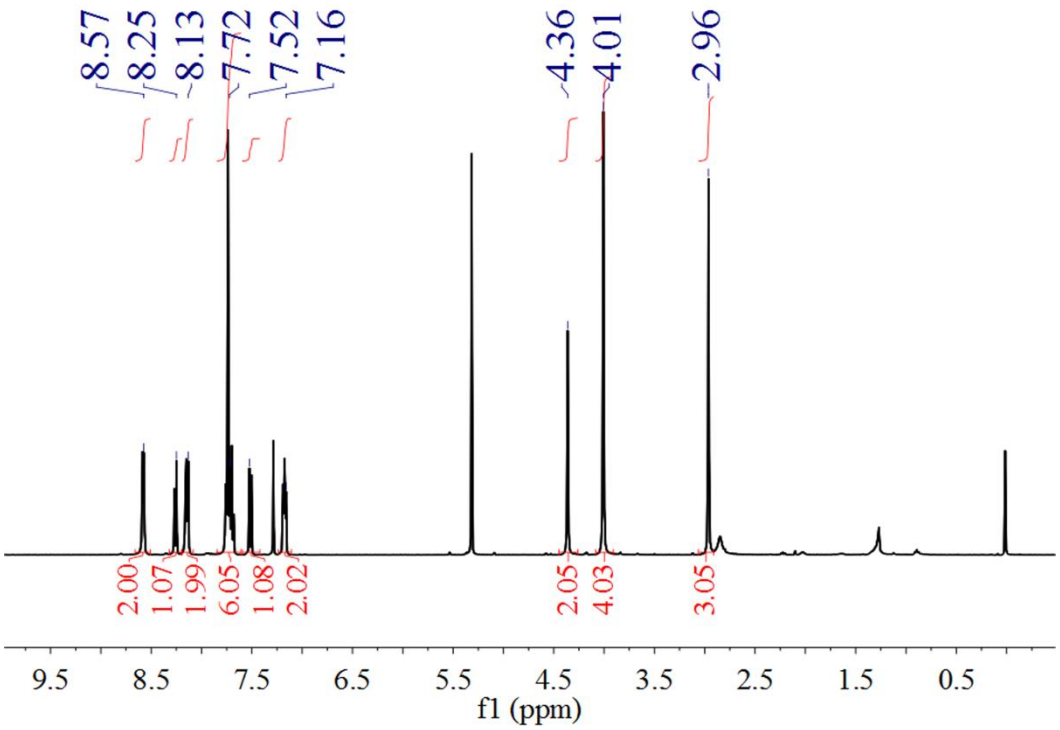

Fig. S1 ^{1}H-NMR of prepared ligand Dmphen-DPA

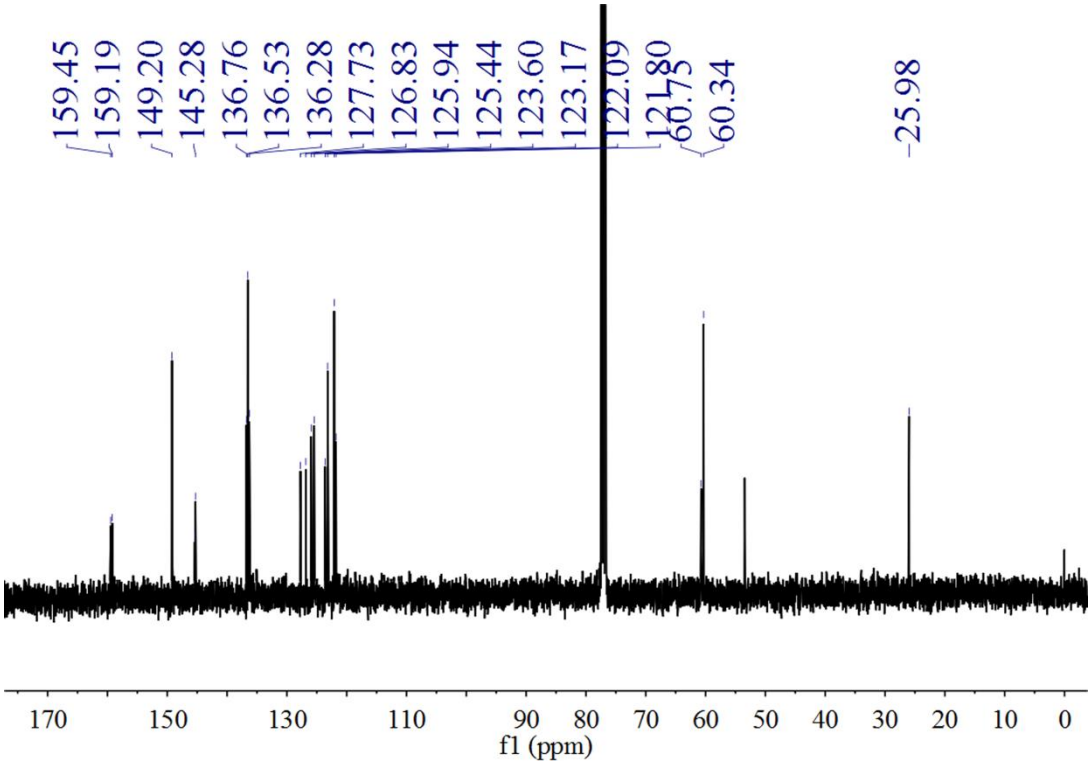

Fig. S2 ^{13}C-NMR of prepared ligand Dmphen-DPA

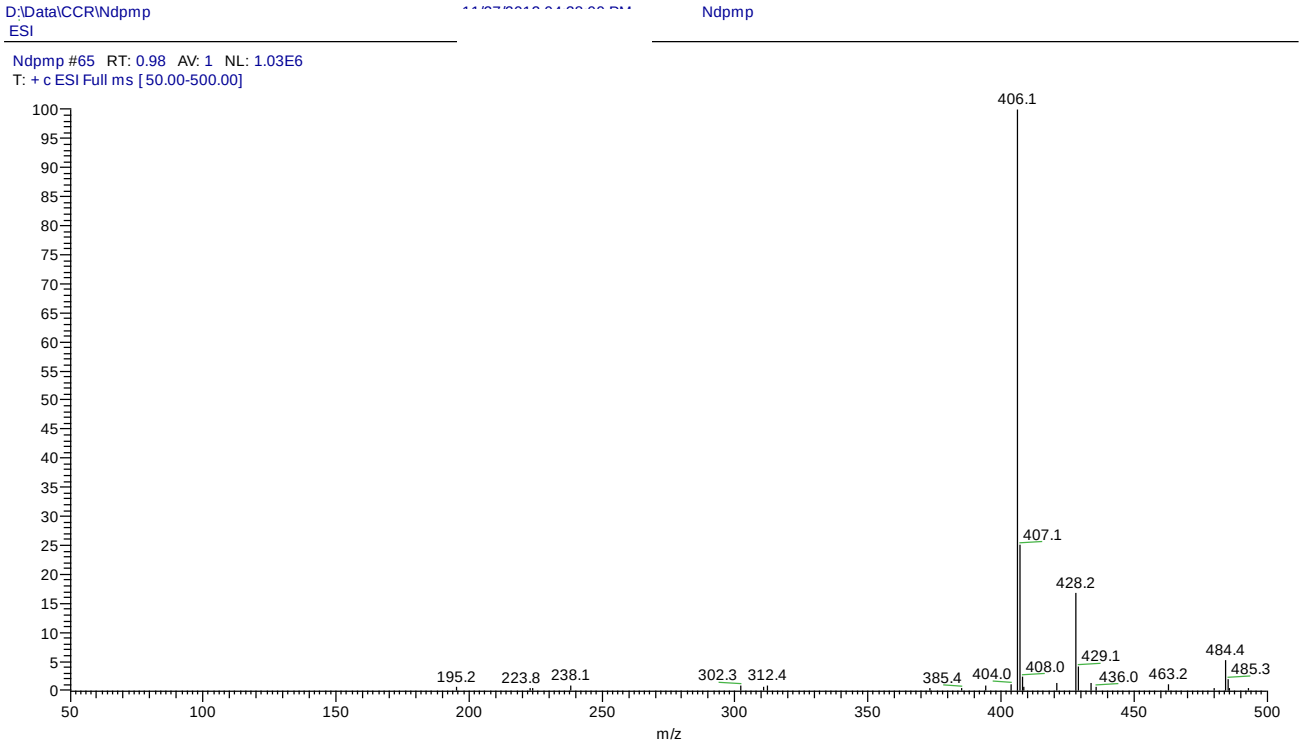

Fig. S3 The ESI-MS spectrometry of ligand Dmphen-DPA.

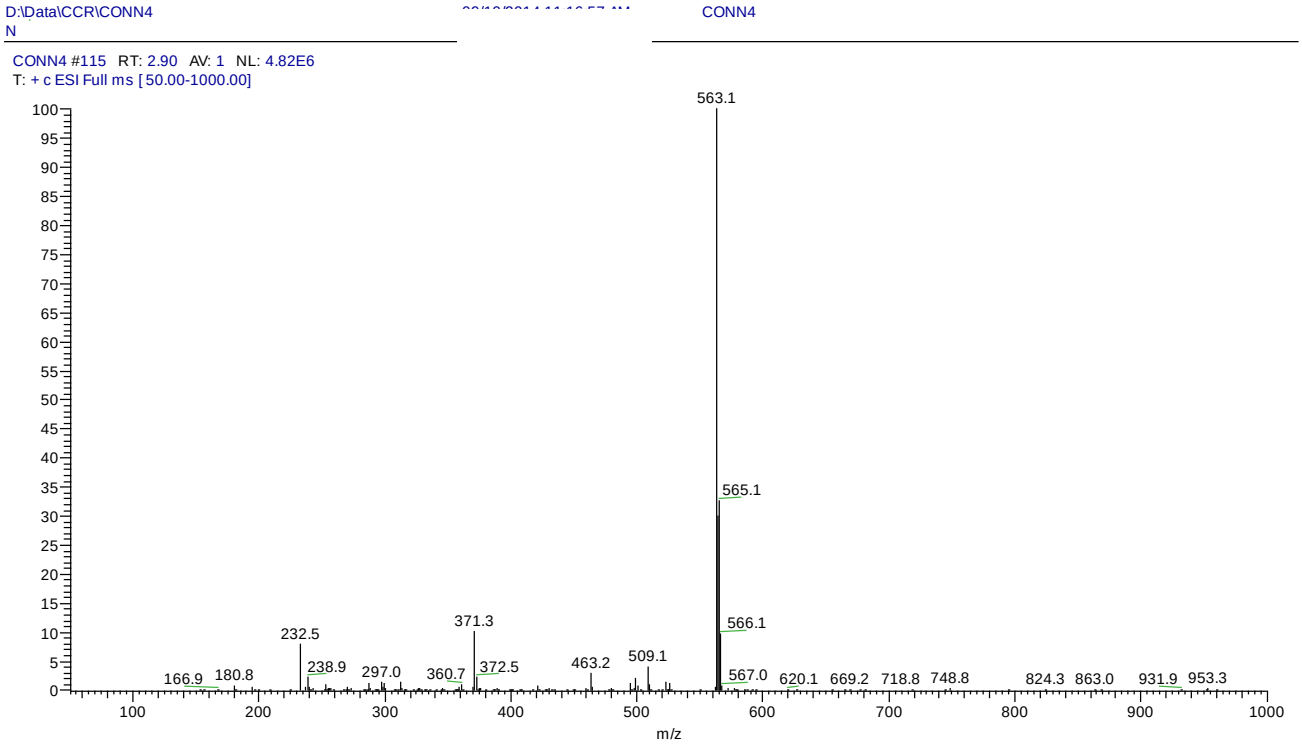

Fig. S4 The ESI-MS spectrometry of complex **1.**

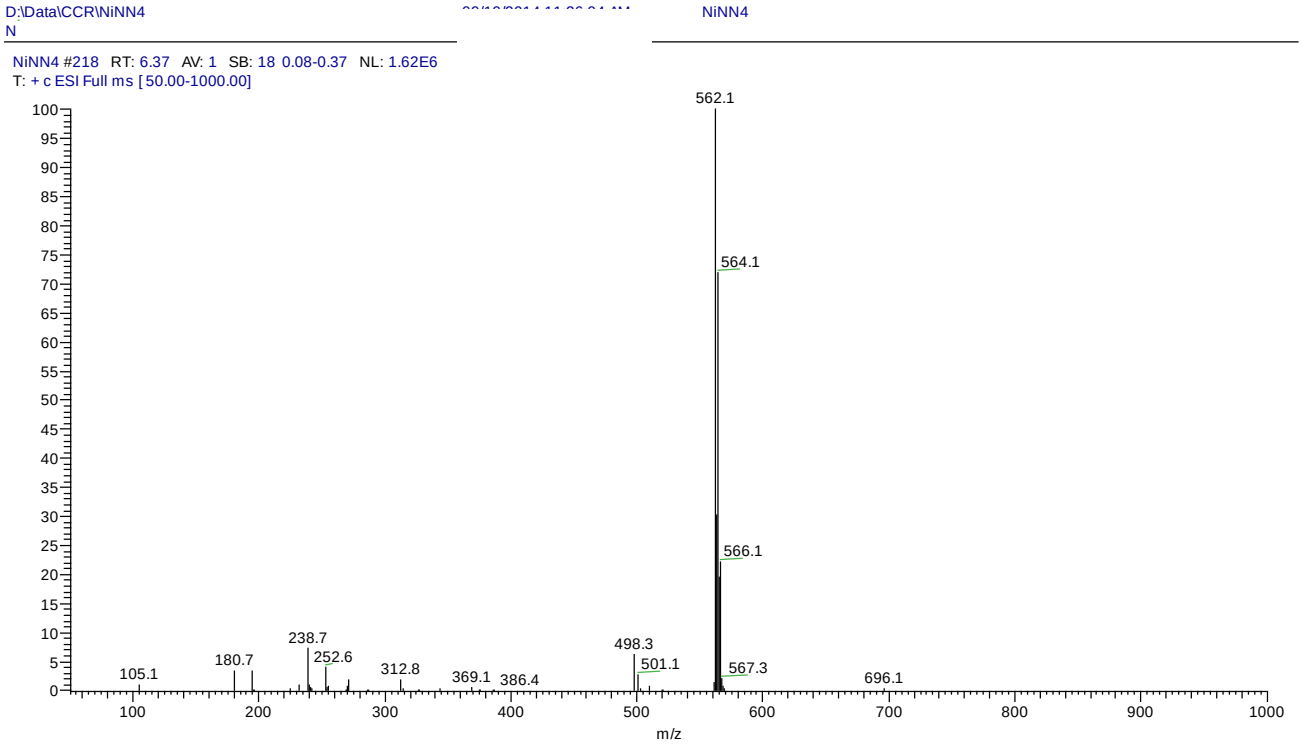

Fig. S5 The ESI-MS spectrometry of complex **2.**

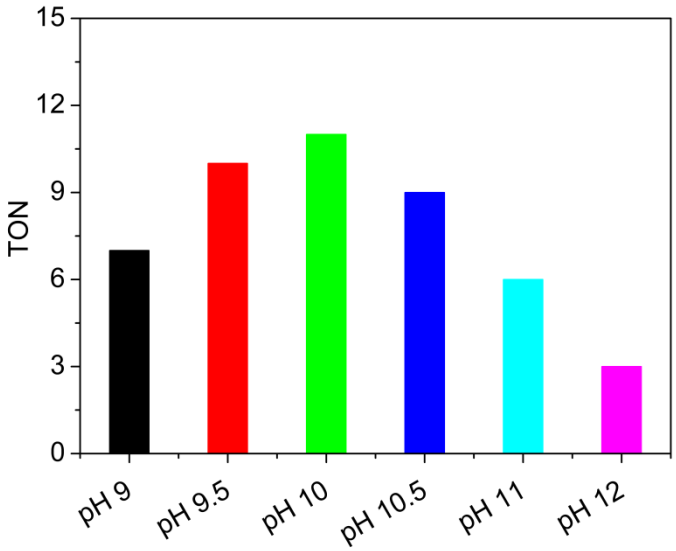

Fig. S6 pH dependence on the hydrogen production over $[Ir(ppy)_2(bpy)]PF_6$/**2**/TEA system under the following conditions: TEA (10 vol%), **2** (0.1 mM) and $[Ir(ppy)_2(bpy)]PF_6$ (0.5 mM) in CH_3CN-H_2O (1/3, v/v) solution; irradiation time 4 h.

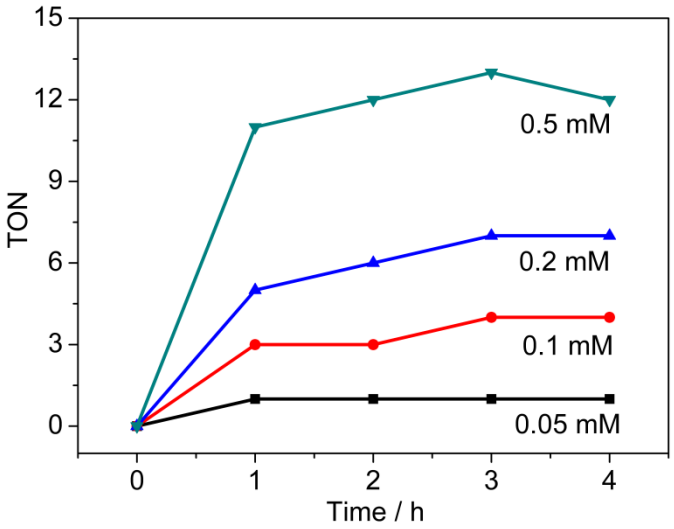

Fig. S7 the dependence of H_2 evolution on the concentration of $[Ir(ppy)_2(bpy)](PF_6)$ from 0.05 mM to 0.5 mM, **2** (0.1 mM), 10 vol% TEA and pH 10 in CH_3CN-H_2O (1/3, v/v) solution.

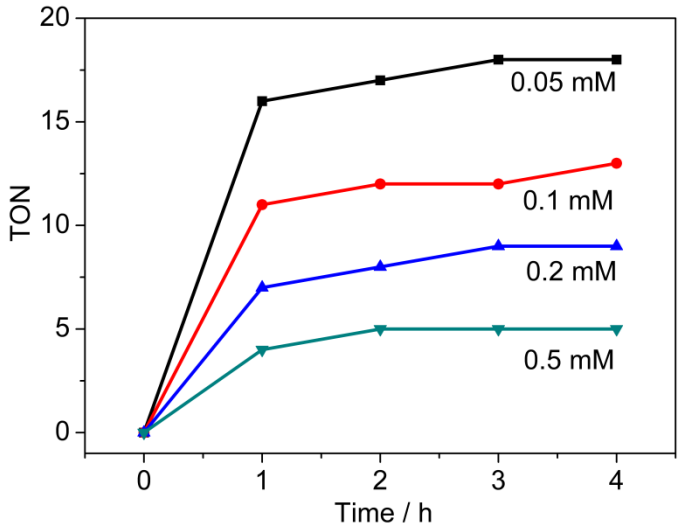

Fig. S8 the dependence of H_2 evolution on the concentration of **2** from 0.05 mM to 0.5 mM, $[Ir(ppy)_2(bpy)](PF_6)$ (0.5 mM), 10 vol% TEA and pH 10 in CH_3CN-H_2O (1/3, v/v) solution.

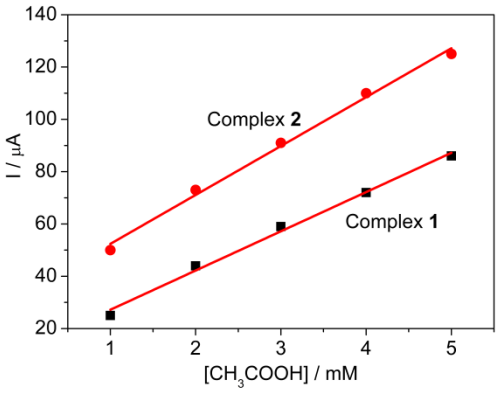

Fig. S9 Acetic acid concentration dependence of the peak current at -2.1 V (*vs.* Fc^{+}/Fc) for complexes **1** and **2**

Table S1 Selected bond lengths (Å) and angles (°) for **1** and **2**

1					
Co(1)-N(1)	2.2153(16)	N(1)-Co(1)-N(3)	77.95(6)	N(2)-Co(1)-O(9)	86.81(6)
Co(1)-N(2)	2.1272(17)	N(1)-Co(1)-N(4)	78.48(6)	N(3)-Co(1)-N(4)	94.86(6)
Co(1)-N(3)	2.1169(16)	N(1)-Co(1)-N(5)	155.36(6)	N(3)-Co(1)-N(5)	103.51(6)
Co(1)-N(4)	2.0414(16)	N(1)-Co(1)-O(9)	100.84(6)	N(3)-Co(1)-O(9)	88.70(6)
Co(1)-N(5)	2.2292(16)	N(2)-Co(1)-N(3)	155.55(6)	N(4)-Co(1)-N(5)	76.88(6)
Co(1)-O(9)	2.0701(14)	N(2)-Co(1)-N(4)	89.32(6)	N(4)-Co(1)-O(9)	176.13(6)
N(1)-Co(1)-N(2)	79.32(6)	N(2)-Co(1)-N(5)	100.91(6)	N(5)-Co(1)-O(9)	103.78(6)
2					
Ni(1)-N(1)	2.150(2)	N(1)-Ni(1)-N(3)	79.63(8)	N(2)-Ni(1)-O(9)	86.27(8)
Ni(1)-N(2)	2.082(2)	N(1)-Ni(1)-N(4)	80.50(9)	N(3)-Ni(1)-N(4)	95.22(9)
Ni(1)-N(3)	2.068(2)	N(1)-Ni(1)-N(5)	158.94(8)	N(3)-Ni(1)-N(5)	102.42(9)
Ni(1)-N(4)	1.982(2)	N(1)-Ni(1)-O(9)	99.02(8)	N(3)-Ni(1)-O(9)	88.27(8)
Ni(1)-N(5)	2.211(2)	N(2)-Ni(1)-N(3)	158.96(9)	N(4)-Ni(1)-N(5)	78.44(9)
Ni(1)-O(9)	2.0683(19)	N(2)-Ni(1)-N(4)	90.05(9)	N(4)-Ni(1)-O(9)	176.32(9)
N(1)-Ni(1)-N(2)	81.19(8)	N(2)-Ni(1)-N(5)	98.59(8)	N(5)-Ni(1)-O(9)	101.99(8)

Table S2 Redox potentials observed in CH_3CN (0.1 M NBu_4PF_6) for complexes **1** and **2**.

complex	$E^{1/2}$ (ox1)	$E^{1/2}$ (red1)	E (red2)[a]	E (red3)[a]
1	-0.02	-1.43	-2.22	-
2	-	-1.42	-2.08	-2.21

[a] Irreversible reduction wave